JOURNAL OF MATERIALS SCIENCE 28 (1993) 3069–3079

Phase equilibria in the Si–C–N–O system and the kinetic analysis of silicon carbide whisker growth

ANIMESH JHA
Department of Materials Technology, Brunel University, Uxbridge, Middlesex UB8 3PH, UK

The significant binary, ternary and quaternary phase equilibria in the Si–C–N–O system are reviewed particularly with regard to the relative stabilities of α and β forms of silicon carbide and nitride. The standard Gibbs free energies of formation of the relevant high-temperature phases are compared, and for the α-form of SiC and Si_3N_4 the values are derived from the empirical results. From these free energy values, the phase boundaries in the Si–C–N–O system have been calculated and are plotted as typical $RT\ln P_{O_2}$ versus $1/T$ plots. The significance of various phase fields in relation to the processing and fabrication of carbide, nitride and oxynitride ceramics is discussed. The rate of chemical reaction has been analysed and the mechanism of reduction of silica to SiC whisker has been proposed. The energetics of whisker growth is also discussed and the derived value of activation energy is compared with the surface self-diffusivity of carbon in pure β-SiC crystals.

1. Introduction

Silicon-based ceramic materials such as silicon carbide (SiC), nitride (Si_3N_4) and oxynitride (Si_2N_2O) have attractive high-temperature properties. These materials retain their strength at elevated temperatures without a significant deterioration in their structural integrity. Strong covalent bonding between the constituent elements in these materials gives rise to a combination of properties such as low thermal expansion coefficient, high Young's modulus and hardness which are important for designing high-performance materials. Consequently these materials have opened new areas in the field of materials design such as those seen in metal- and ceramic-matrix composites. Currently, the fabrication cost of these novel engineering materials is high, partly due to the cost of production of raw materials used in designing the matrix and reinforcements.

Carbothermic reduction of silica under a controlled atmosphere can yield silicon carbide, nitride and oxynitride. This method has also been employed for producing ceramic whiskers which are used as a reinforcement in a suitable ceramic matrix. Several studies in the past have been undertaken to synthesize SiC, Si_3N_4, Si_2N_2O and silicon–aluminium oxynitrides (sialons) [1–9]. Specific ways of controlling the partial pressures of reactive gases during the carbothermic reduction of silica have been shown particularly to form ceramic whiskers [2, 3, 7].

The present investigation elucidates the governing phase equilibria in the Si–C–N–O system by reviewing the significance of binary and ternary phase relationships. The thermodynamic stability of the relevant ceramic phases in powder and whisker forms that can be produced simultaneously in a reduction process are emphasized. We also discuss the kinetic analysis for the reduction of silica to SiC and the mechanism of growth of ceramic whiskers in the presence of iron impurities. The governing diffusion-controlled process is also analysed and its temperature coefficient is determined to estimate the rate of whisker growth.

2. Phase relationships in the Si–C–N–O system

2.1. Binary Si–C and Si–N phase equilibria

The attractive high-temperature properties of silicon carbide led to an extensive investigation of the phase relationship between silicon and carbon. One of the earliest works was reported by Chipman *et al.* [10] in 1954, in which the solubility limits of Si and C in an Fe–Si–C alloy were established. The timely development of silicon metal as a material for semiconductors initiated an expansion of interest in this field and it was then realized that silicon carbide could well be a high-temperature semiconductor material. A complete symposium proceedings edited by O'Connor and Smiltens [11] in 1960 was devoted to this subject. These proceedings cite several articles on the phase equilibria in the Si–C system. Using a mass spectroscopic technique, Drowart and De Maria [12] measured the heat of formation of SiC species and reported that the enthalpy at 298 K, ΔH°_{298}, is equal to -473 ± 13 kJ g-atom^{-1} for the Si(g) + C(gr) = SiC(hex) reaction where (g) and (gr) represent the gaseous phase and graphite, respectively. SiC(hex) is known as the hexagonal form of the β-SiC which has an f.c.c. structure. This led to evaluation of the ΔH°_{298} value for the

reaction Si(s) + C(graphite) → SiC(hex) which is -76 ± 13 kJ mol^{-1}. This value is in good agreement with the standard Gibbs free energy data compiled by Turkdogan [13] which are for the β-phase. It is pointed out that Drowart and De Maria did not ascertain the structure of the silicon carbide phase.

On the other hand, Scace and Slack [14] measured the solubility of carbon in liquid silicon at 35 atm of argon gas and found that the SiC phase melts incongruently at 3103 ± 40 K. The heat of solution of carbon in liquid silicon is 247 kJ mol^{-1}. From this investigation, the equilibrium solubility of C in liquid silicon at its melting point is 5×10^{-3} at%, which rises to 19 at % C at the decomposition temperature of SiC. Based on the measurement of carbon solubility in liquid silicon and by using the Czocharalski method, Halden [15] grew β-SiC crystals from pure liquid silicon and a 30 wt % Si-containing iron silicide liquid. No growth of α-SiC crystals was reported under these conditions. The stability of β-SiC under these conditions will become apparent when the oxygen potential diagrams are discussed below.

The complete Si–N phase equilibrium is not fully understood, but it is well known that the compound Si_3N_4 exists. The Gibbs free energy for the formation (ΔG°) of this phase was determined by Pehlke and Elliott [16] using dissociation pressure measurements, from which it was established that for the reaction

$$3Si(s) + 2N_2(g) = Si_3N_4(s) \quad (1)$$

the value of ΔG° is equal to $-874\ 247 + 405T$ J mol^{-1} of Si_3N_4. This free energy value was believed to define the equilibrium of a mixture of α and β silicon nitrides. Wild *et al.* [17] subsequently confirmed that the value of standard Gibbs free energy change reported by Pehlke and Elliott is for the β-form of silicon nitride. It was also pointed out that a considerable amount of difficulty might exist in obtaining a single-phase silicon nitride in either α or β form by nitriding silicon metal. This was illustrated on the basis of an isothermal predominance area diagram by Wild *et al.*

2.2. Ternary Si–C–O and Si–N–O phase equilibria

Some of the earliest work to establish the phase equilibria in the Si–C–O system was reported by Krivsky and Schumann [18], who detailed the prevalent condition in a typical silicon blast furnace. This work particularly points out the problems that can possibly occur inside a silicon blast furnace. With the rising demand for silicon metal, further work was also carried out in this area and Rosenqvist [19] on the basis of results reported by Schei [20] pointed out the features of the univariant and invariant reactions in the Si–C–O system for the reduction condition in a silicon blast furnace. The underlying requirements for maintaining the stoichiometry of the metal-making reaction were stressed, since otherwise this would lead to a severe loss of SiO gas from the vertical furnace. The above workers [18, 19] recognized the significance of the stability of the SiC phase in an SiO, CO and CO_2 gas mixture in the temperature range 1573 to 2373 K.

In recent years, SiC has been recognized as a high-temperature ceramic material. Apart from the carbothermic reduction technique, which of late has also gained interest, there are two other popular methods, one of which particularly claims to produce high-quality ultrafine silicon carbide powder. The first reaction is the thermal dissociation of a mixture of silicon tetrachloride vapour and methane gas, which yields SiC microcrystalline powder and HCl gas [21]. The other is based on the synthesis and polymerization of a silicon organometallic compound. This method was first developed in Japan by Yajima *et al.* [22] and has now become an established commercial route for the fabrications of nicalon-type SiC ceramic fibres. In this method, the metal-organic dimethyl dichlorosilane, which is an aliphatic liquid, is dechlorinated with an alkali metal such as Li, Na or K. The dechlorination is thermodynamically possible because the C–Cl bond in the aliphatic chain structure is at a higher chemical potential than the M–Cl bonds in alkali chlorides. Removal of chlorine from the aliphatic chain encourages a simultaneous polymerization reaction leading to the formation of a polycarbosilane liquid at 623 K which is then melt-spun to produce fibres that are cured at 463 K.

On the other hand, the carbothermic reduction of silica utilizes cheap raw materials and sufficient data are available which suggest that the method can be employed for the production of both SiC powder and sub-micrometre and larger-size whiskers [1–3, 7, 8]. A significant proportion of this paper is devoted to the aspects of growth of SiC crystals and these are described below. There are two allotropic forms of silicon carbide: the form having a zinc-blende structure which is called β-SiC (3C-type) and the hexagonal modification (α-SiC) which is related to the cubic arrangement by rotation of the tetrahedral SiC units in alternating layers in either parallel or antiparallel orientation. The latter has various polytypes that differ in the stacking sequence of the silicon and carbon layers, and on this basis the 6H form is the most stable polytype of α-SiC with a c axis of 1.56 nm, i.e. six times the Si–C distance (0.251 nm). The other less stable forms are 4H and 21R where the c axes are also multiples of the SiC bond distance. A few structural investigations of α-SiC [23, 24] have concluded that polytypes of higher orders reaching up to 141R are also possible. It was reasoned that the origin of polytypism in the hexagonal form is a consequence of a long-range order structure along the c direction. The stability, stacking sequence using Ramsdell notation and the c dimensions of a few α-polytypes are shown in Table 1. On the basis of thermodynamic and kinetic data, the origin of polytypism in the α-form is also examined below. Indeed the two predominant crystallographic forms also have different values of the optical and electronic band gaps (see Table I).

The phase equilibria in the Si–N–O system were investigated by Wild *et al.* [17], who determined the isothermal predominance phase fields by constructing oxygen–nitrogen potential diagrams. The relevant

TABLE I Polymorphs and polytypes of silicon carbide and their cell dimensions and band gaps

Property	β-SiC (cubic)	α-SiC (hexagonal) Ramsdell notation	a (nm)	n	$c = 0.2512n$ (nm)
Cell dimension					
	$a = 0.434$ nm	4H	0.3073	4	1.005
	(3 C type)	6H	0.3073	6	1.508
		15R	0.3073	15	3.770
		21R	0.3073	21	5.278
		33R	0.3073	33	8.294
		51R	0.3073	51	12.818
Band gap (eV)					
Electronic	1.90	2.80			
Optical	6.0	6.20			
Decreasing order of stability 6H > 4H > 15R.					

phase relationships were established by equilibrating an Fe–14 wt % Si alloy with an H_2, NH_3 and H_2O gas mixture in a narrow temperature range. The experimental data were compared with other reported results and were found to be in good agreement. Wild *et al.*, on the basis of their thermodynamic measurements and their comparison with the data obtained by Pehlke and Elliott [16], pointed out a difference in the free energy difference between the two forms of silicon nitrides. Colquhoun *et al.* [25] subsequently reported that β-Si_3N_4 is the pure form which is made up of covalent SiN_4 tetrahedra joined in a three-dimensional network by sharing corners; each nitrogen corner is common to three tetrahedral units. The details of the structural arrangement in silicon nitride were extensively discussed by Wild *et al.* [26]. In the structure of α-Si_3N_4, it was reported that one oxygen atom replaces every 30 nitrogen atoms in an array of SiN_4 tetrahedra. The presence of oxygen atoms in the structure, as stated above, accounts for an obvious difference in the stability of α and β silicon nitrides. If this is so, from the molar enthalpy and entropy of formation of SiO_2 and Si_3N_4 (β), the free energy difference between the α and β forms could be estimated. Since in the α-Si_3N_4 structure the probability of finding an oxygen atom in place of a nitrogen atom is 1/30, the standard Gibbs free energy change for the reaction Si_3N_4 (β) + $3(O)_2 = 3SiO_2$ (quartz) + $2N_2$(g) should be multiplied by this oxygen occurrence factor (the calculated value of ΔG° is $-1\,996\,964 + 212.1T$ $J mol^{-1}$ of Si_3N_4 [16, 25]). At 1567 K this value is $-55\,488$ J. This should be the free energy for one SiO_4 tetrahedron in an array of 30 Si_3N_4 tetrahedra. Because each oxygen is expected to be tetrahedrally coordinated, the free energy per unit Si–O bond is $-13\,872$ J which appears to be in satisfactory agreement with the difference of $-13\,385$ J reported by Wild *et al.* at 1567 K. This apparent difference in ΔG°, arising from the substitution of an Si–N bond by Si–O, is summarized in Table III, by the reference of Table II.

The occurrence of polymorphism in silicon nitride could therefore be accounted for by the presence of oxygen in the structure. In Tables II and III the free energy data for α and β silicon nitrides and silicon oxynitrides are summarized and the difference in their ΔG° values is evident in Fig. 1. From these tables it is evident that the difference in the values calculated by using two sets of measured data [16, 17] for the stability of β-Si_3N_4 is less at lower temperatures than at a higher T. The empirical values, however, are significantly different at high T due to a larger value of error incorporated with the measured data.

2.3. Si–C–N–O phase equilibria

The estimation of phase boundaries in Si–C–N–O requires the values of standard Gibbs free energies of formation of binary and ternary phases discussed above. A few interpretations of the phase boundaries are discussed below, one of which was computed by Wada *et al.* [8] using the thermodynamic data from the Journal of Army, Navy and Air Force (JANAF) and of Wild *et al.* for the β-Si_3N_4 phase. The chemical potential versus temperature diagram in the Si–C–N–O system is re-evaluated using the binary Gibbs free energy data for quartz, β-SiC and β-Si_3N_4 from the thermodynamic data compilation of Turkdogan [13] and the Gibbs free energy of forma-

TABLE II Summary of standard Gibbs free energy of formation of α and β silicon nitrides and silicon oxynitrides

Reaction	ΔG° (J)	Source reference
$3\{Si\} + 2(N_2) = \langle \beta\text{-}Si_3N_4 \rangle$	$-874\,540 + 405T$	[16]
$3\{Si\} + 2(N_2) = \langle \beta\text{-}Si_3N_4 \rangle$	$-962\,413 + 477T$	[17]
$\frac{11.4}{4}s\{Si\} + \frac{7.5}{4}s(N_2) + \frac{0.15}{4}s(O_2) = \frac{1}{4}s\langle Si_{11.4}N_{15}O_{0.3} \rangle$	$-1029\,363 + 515T$	[17]
$2\{Si\} + \frac{1}{2}(O_2) + (N_2) = \langle Si_2N_2O \rangle$	$-1200\,924 + 494T$	[17]

TABLE III Calculated values of ΔG°_β from Table II and estimated values of ΔG°_α per Si–O bond from the standard Gibbs free energy change[a] for the reaction $\langle\beta\text{-}Si_3N_4\rangle + 3(O_2) = 3\langle SiO_2\rangle_{quartz} + 2(N_2)$

T (K)	ΔG° (J) for β-Si_3N_4		$\beta \rightarrow \alpha$ transformation (J)		
	Wild *et al.* [17]	Pehlke and Elliott [16]	Wild *et al.* [17]	Pehlke and Elliott [16]	Empirical [25]
1000	− 485 344	− 472 792	− 59 011	− 59 509	–
1400	− 294 554	− 307 440	− 57 141	− 56 680	–
1473	− 256 898	− 258 813	− 56 763	− 56 167	− 63 597
1523	− 237 651	− 242 999	− 56 528	− 55 813	− 53 555
1573	− 210 455	− 227 246	− 56 292	− 55 460	− 43 514
1600	− 199 158	− 226 438	− 56 209	− 55 266	–
1623	− 186 188	− 211 493	− 56 058	− 55 106	− 43 514

[a] The values of standard Gibbs free energy change for each SiO_4 tetrahedron in an array of 30 SiN_4 tetrahedra are $-66\,581 + 7.07T$ [16] and $-63\,686 + 4.7T$ [17].

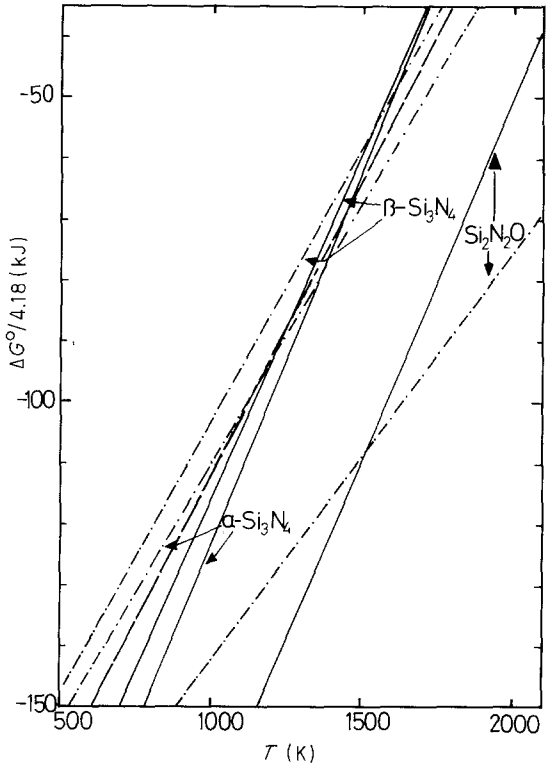

Figure 1 Plots of standard Gibbs free energies of formation (ΔG°) of α and β silicon nitrides and oxynitrides against absolute temperature: (——) experimental ΔG°, (— · —) theoretical entropy plus average experimental ΔG°, (— —) Pehlke and Elliott [16].

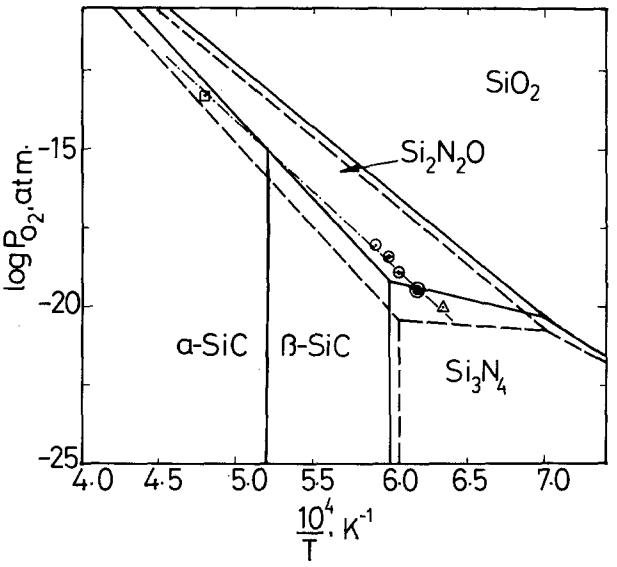

Figure 2 Comparison of (——) the present Si–C–N–O equilibria with (– – –) those of Wada *et al.* [8]; (⊡) Li *et al.* [27], (⊙) Milewski *et al.* [3], (⊙) Wada *et al.* [8], (△) de Jong *et al.* [28].

tion of the ternary oxynitride phase from Wada *et al.* The differences in the computed phase boundaries and invariant points are evident in Fig. 2.

A few investigators [27–29] have reported the formation of α-SiC during the carbothermic reduction of silica. A particular illustration of the change in morphological characteristics was also emphasized by Milewski *et al.* [3]. From the results for the composition of the exit gas phase [3, 8, 27, 28], the value of oxygen partial pressure in equilibrium with the hexagonal form of SiC can be estimated. These values of P_{O_2} are plotted in Fig. 2 against the reciprocal of the absolute temperature, and from the $RT\ln P_{O_2}$ versus $1/T$ relationship the values of slope and intercept of the best-fit straight line joining these points were derived. From the equation of the best-fit straight line which represents the α-SiC → Si_2N_2O univariant given by the reaction:

$$2SiC(hex) + (N_2) + 1/2(O_2) = Si_2N_2O + 2C \quad (2)$$

the standard Gibbs free energy change (in J mol^{-1}) of N_2 gas is $-366\,167 + 40.3T$ ($\pm$ 25 kJ). In all the above set of data, where predominantly β-SiC phase was observed, it was also reported that a substantial part of the reaction product had a widely different morphology and colour. This could only be due to the presence of impurities such as N_2 and O_2 which were either intentionally incorporated in the gas phase mixture or present as the residual volume in the bulk gas mixture. A few experiments have also been carried out in this investigation under controlled oxygen potential, and these data points at 1648 and 1698 K are shown in Fig. 2; there is an apparent variation amongst the data obtained in this investigation and previously reported gas compositions in which the 2H-type hexagonal form was often observed.

The powder diffraction results obtained in the present work suggest the presence of 12H-type hexagonal

phase. In Fig. 3 a standard 12H-type α-SiC powder diffraction pattern is compared with our results. By examining the X-ray powder diffraction pattern where the strongest lines are due to {1 1 1}, {2 2 0} and {3 1 1} family of planes, one can wrongly deduce that these diffraction vectors are related, i.e. $d_{(1\,1\,1)} + d_{(2\,2\,0)} = d_{(3\,1\,1)}$ to give β-SiC single-crystal growth. Clearly this is not the case since there are weaker peaks in the powder diffraction pattern, and combined with the above crystallographic planes can be possible from α-SiC (12H-type) crystals. It should be noted that the β → α transformation is a kinetically controlled process, and often several days are needed to achieve complete conversion [30]. Our experiments were run typically for 30 h. Pure β-SiC is of dark grey or black colour, and only when other polytypes start forming due to a variation in the local gas composition, does the colour of SiC change. Such a variation in appearance arises due to a small change in the band gap of the hexagonal form of silicon carbide. Some evidence in the literature exists for such a variation [3, 4]. Such a compositionally-sensitive morphological variation in silicon ceramics is quite common, and has also been observed when silicon nitride whiskers are produced [4, 17]. Illustrations of the compositional dependence of morphological variation in Si_3N_4 and metallic copper whiskers have been cited elsewhere by Wild *et al.* and Jha and Grieveson [26, 31], respectively. The former have shown an "unmistakable" difference in two forms of α-SiN, whereas the latter authors in some of their earlier work on copper whiskers have shown that wide-ranging morphologies arise due to compositional fluctuation in the gas phase [31].

It is interesting to note that there is some similarity between the β and α forms of SiC and Si_3N_4, the latter two being prevalent phases in an oxygen-rich atmosphere. Invoking the comparison of H° values discussed above [12, 13], the apparent difference between these two values could arise from the specific heat correction applied to the measured room-temperature enthalpy. In the light of these two data, which also agree with the JANAF thermodynamic data ($-72\,832 + 7.0T$), the free-energy equation for the formation of β-SiC from Turkdogan [13] can be reliably accepted. From the derived values of slope and intercept for the univariant represented by Equation 2, the free energy of formation for the wurtzite form of SiC, i.e. Si(s) + C(gr) = α-SiC(s), is $-146\,066 + 45.47T$ J mol^{-1}. The error in ΔG° is of the order of ± 25 kJ per mole. This then yields the value of ΔG° for β → α transformation, which is equal to $-73\,031 + 37.81T$ J, the equilibrium temperature being 1930 K. In Fig. 2, the equilibrium values of oxygen partial pressure for 12H-type α-SiC are plotted and these vary considerably from the tentative univariant line defined by Equation 2. This may arise from the possibility of a range of stability over which other polytypes might exist on the oxygen potential diagram.

In the light of the above derivation of the free energy, it is understandable that the β-SiC is a low oxygen potential allomorph which can transform to wurtzite in the presence of oxygen impurities. To what extent the transformation is affected by other impurities such as nitrogen is not well understood. Indeed this is also the reason that extensive carburization of either pure metallic silicon or iron silicide yields β-SiC crystals, because the metallic silicon keeps the partial pressure of oxygen well below the critical value required for the β → α transformation.

It should be noted that the β to α transformation in SiC has a negative enthalpy, and this change demonstrates that the hexagonal form has a significantly large structural order in the *c* direction [23, 32, 33] which is also the direction of the predominant Si–C bonding. The enhanced order in the wurtzite structure

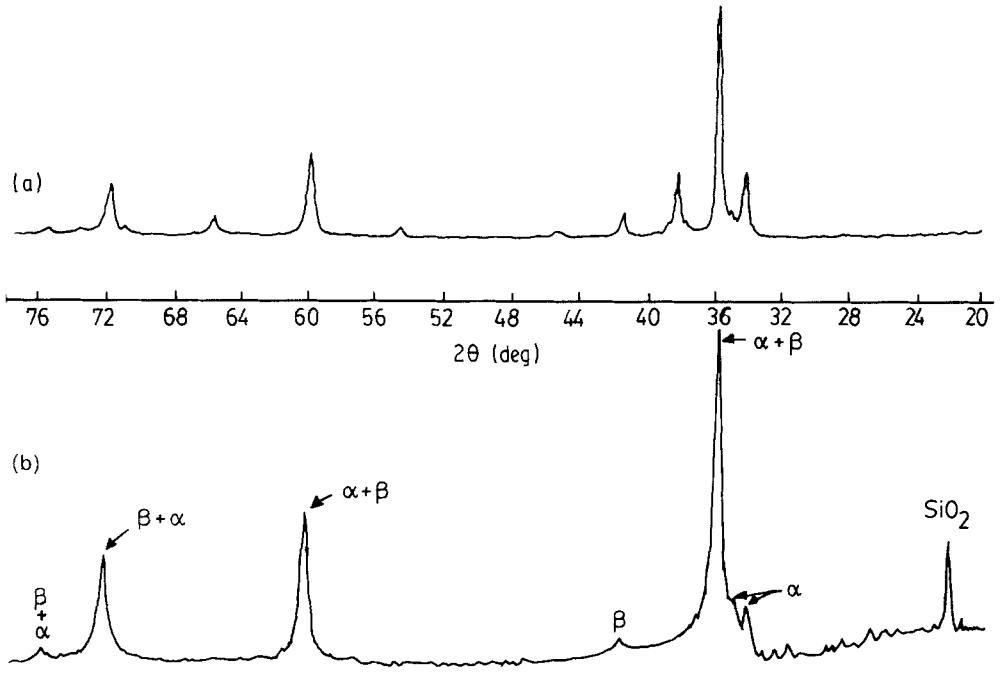

Figure 3 Comparison of X-ray powder diffraction patterns of (a) a standard 12H-type α-SiC with (b) the present α-SiC + β-SiC produced by equilibrating the SiO_2–C mixture with an Ar–H_2–H_2O–CO–CO_2 gas mixture in equilibrium with Fe–FeO.

can be ascribed to a further extension of SiC units along the close-packed c axis in the presence of impurities because the enthalpy data primarily represent the Si–C bonding. On this basis, a systematic arrangement of impurity atoms in the ordering direction leading to a net decrease in the entropy of the wurtzite structure is expected (cf. the ΔG° value for the α form). The level of oxygen or impurity atom in the structure could not be estimated from the above phase relationships. However, there are a number of citations in the literature to the effect that clustering of oxygen on the surface of β-SiC whiskers and in the grain boundary regions occurs extensively. Allard *et al.* [30] have recently confirmed the preferential concentration of oxygen on the surface of β-SiC crystals.

The value of ΔH° derived from the graphical relationship indicates that the value of enthalpy for α-SiC is twice as large as for β-SiC, and there is also a net decrease in the overall entropy of the wurtzite structure. This is expected in the light of transmission electron microscopic evidence, which points towards ordering in the c direction. It is therefore worth pointing out that the 3C type (β-SiC) is structurally related to the 6H type (the stablest polytype of wurtzite) since 6H and 12H are of the same type. Here C and H are the directions of close packing.

Several transmission electron microscopic investigations [23, 24, 30, 34] on the $\beta \rightarrow \alpha$ transformation in polycrystalline SiC suggest that without the extensive long-range "ordering" completely disordered α-SiC crystal might form. The possibility of incorporation of Si–O tetrahedra in the SiC structural array could give rise to an extended order, since both structural units are compatible with each other provided some distortion could be allowed, a point made by Amelinckx and Strumane [35].

2.4. Recalculation of the Si–C–N–O phase relationship

Recalculation of the significant phase equilibria in the Si–C–N–O system has become necessary because the previous relationship in Fig. 2 precludes the α-form of silicon carbide and nitride which are frequently observed during the hot pressing of the ceramic phase. The free energy data for the determination of the phase boundaries were selected from the empirical data of Wild *et al.* [17] and Colquhoun *et al.* [25]. Based on their thermodynamic measurements, the free energies of formation of the nitrides and oxynitride phases were derived. The latter authors also commented on the accuracy of the measured data and rederived a set of values by combining the appropriate theoretical entropy term with the average of the empirically derived enthalpy values in the range 1473 to 1623 K. These free energy values are summarized in Table IV together with the chemical reactions representing various significant phase equilibria in the Si–C–N–O system. The activity of carbon and the partial pressure of nitrogen gas for the computation of phase boundaries are considered to be unity.

Using the empirical entropy value from [25] and Equation 2, the calculated phase stability diagram is shown in Fig. 4. However, if the theoretical entropy value is considered for the formation of nitrides and oxynitride phases, then the stability range of the α-phase becomes much larger than has been observed empirically. This is supported by earlier experimental evidence where Colquhoun *et al.* pointed out that the α phase could not exist as a single phase above 1573 K. At 1 atm of nitrogen pressure, the α-phase field closes at ~ 1500 K, which is lower than predicted from the Si–N–O predominance diagram [36]. However, such a difference could also arise from the values of thermodynamic data being selected from different sources. The univariant diagram clearly predicts that the α form of silicon nitride is a low temperature and high oxygen potential phase, and is consistent with the experimentally determined phase predominance diagram. It is also pointed out that incorporation of the theoretical entropy term with the experimentally determined enthalpy data for nitrides and oxynitrides exaggerates the stability range of α-

TABLE IV Standard Gibbs free energy change (ΔG_T°) in the Si–C–N–O system

Reaction	ΔG_T° (J)
$\frac{11.4}{4}\langle SiC\rangle_\beta + \frac{7.5}{4}(N_2) + \frac{0.15}{4}(O_2) = \frac{1}{4}\langle Si_{11.4}N_{15}O_{0.3}\rangle + \frac{11.4}{4}\langle C\rangle$	$-676\,855 + 407.38T$
$\langle Si_2N_2O\rangle + \frac{3}{2}(O_2) = 2\langle SiO_2\rangle + (N_2)$	$-714\,289 - 82.24T$
$\frac{3}{4}\langle Si_{11.4}N_{15}O_{0.3}\rangle + 0.15(N_2) = \frac{11.4}{4}\langle Si_3N_4\rangle + \frac{0.45}{4}(O_2)$	$345\,097 - 184.5T$
$\frac{1}{4}\langle Si_{11.4}N_{15}O_{0.3}\rangle + \frac{5.4}{4}(O_2) = \frac{5.7}{4}\langle Si_2N_2O\rangle + \frac{3.6}{8}(N_2)$	$-681\,724 + 188.86T$
$2\langle SiC\rangle_\beta + (N_2) + \frac{1}{2}(O_2) = \langle Si_2N_2O\rangle + 2\langle C\rangle$	$-953\,389 + 418.3T$
$\frac{1}{4}\langle Si_{11.4}N_{15}O_{0.3}\rangle + \frac{11.25}{4}(O_2) = \frac{11.4}{4}\langle SiO_2\rangle + \frac{7.5}{4}(N_2)$	$-1699\,586 + 69.85T$
$\langle SiC\rangle_\beta + (O_2) = \langle SiO_2\rangle + \langle C\rangle$	$-833\,839 + 168T$

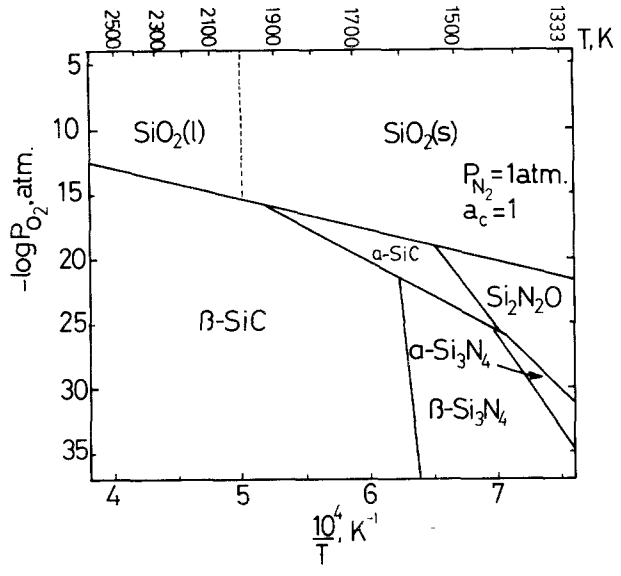

Figure 4 Re-calculated Si–C–N–O phase equilibria with α-SiC and Si_3N_4 phases with relevant line for α-SiC from Fig. 2.

Si_3N_4, and therefore is inconsistent with the empirical data thus far reported.

The computed Si–O–C–N phase equilibria can be applied in understanding the development of microstructure in silicon-based ceramics. For example, the equilibrium microstructure evolution during sintering of silicon nitride powder can be predicted using the phase relationship shown in Fig. 4. One of the earliest examples was given by Colquhoun *et al.* [25]. The significance of surface SiO_2 in determining the SiO pressure was described by Colquhoun *et al.* and it was emphasized that when the SiO pressure is high, the α phase forms because the higher SiO partial pressure also corresponds to an equivalently higher oxygen potential in the system. Above 1500 K, from Si–C–N–O phase stability diagram, α-Si_3N_4 will no longer be in equilibrium with either the β phase or oxynitride. Therefore during hot pressing under a given oxygen partial pressure if the α-phase remains stable, the extent of its metastability could be determined either with respect to oxynitride or the β-Si_3N_4 univariant line in Fig. 4.

Further details also emerge when the formation of an oxynitride glassy phase is considered from which the nucleation of β-Si_3N_4 crystals occurs. The stability of the silicon oxynitride can be also understood from this phase diagram because neither the invariant point nor the concurring univariants are related to the stability of the α phase. It is evident that when the temperature during slow cooling of an oxynitride melt falls below 1500 K, the α phase should form. Evidently this is true for a strictly ternary silicon nitride (α + β) and oxynitride system. In the presence of low-viscosity liquid-forming additives such as MgO, CaO etc., the thermodynamic activity of silica in the oxynitride melt is considerably lower than unity. The lower value of a_{SiO_2} in the melt is therefore equivalent to a much reduced partial pressure of oxygen in equilibrium with the oxynitride melt. MgO dissolved in the oxynitrides usually forms a forsterite phase (Mg_2SiO_4) as observed by Sun *et al.* [37]. Sun *et al.* also pointed out that during the slow cooling, the α form nucleates from the liquid phase in the temperature range 1273–1673 K. If, however, the temperature is raised above 1673 K, the α → β transformation commences. This proves that in the MgO-containing oxynitride liquid, the value of oxygen potential is not sufficiently low to encourage the reconstructive α → β transformation. The reaction is critical for enhancing the strength of the ceramic phase, which can be achieved in practice by controlling the oxygen potential so that there is a sufficient driving force for a diffusion-controlled phase transformation. By adopting this technique, the phase transformation can be initiated in the temperature range where the α phase is quite stable.

Finally, the oxygen potential diagram also explains the extended stability of the oxynitride phase which also plays a critical role in determining the microstructure of the silicon nitride ceramics, particularly the grain-boundary glassy phase. It is worth noticing that in view of the above empirical evidence it is impossible to predict the evolution of α-Si_3N_4 phase from Fig. 2.

3. Kinetics of silicon carbide formation

3.1. The gaseous reaction

The critical reactions necessary for the formation of silicon carbide powder and whiskers were described in our earlier work [7] where the two competing reactions defined below were discussed. The first reaction is the reduction of liquid or solid silica to produce a gaseous mixture of carbon and silicon monoxides, i.e.

$$SiO_2(s) + C(gr) = (SiO) + (CO) \quad (3)$$

Because the direct reduction of SiO_2 to SiC is kinetically less favourable and mechanistically impossible after the initial state due to the loss of a physical contact between carbon and SiO_2, the reduction of SiO with carbon is a more dominant course of reaction for the formation of SiC crystals. In this step, the SiO gas produced from Reaction 3 is consumed to yield SiC and CO gas. The indirect reduction of SiO_2 and SiO with CO leading to the formation of whiskers is thermodynamically less likely because of the higher stability of CO_2 gas at temperatures below 1273 K. Also, if any CO_2 is locally present within the pore volume it will be expected to convert into CO via $C + CO_2 = 2CO$. The silicon carbide formation reaction is therefore

$$(SiO) + 2C(gr) = \beta\text{–}SiC + (CO) \quad (4)$$

The equilibrium values of CO and SiO can be estimated from the standard Gibbs free energy equations for Reactions 3 and 4, and are equal to $688\,354 - 344T$ and $-83\,242 + 4.7T$ J mol^{-1} of CO gas, respectively. Evidently the stoichiometry of Reactions 3 and 4 requires that the flux of SiO (J_{SiO}) should be related to that of the CO gas. Hence for the formation and consumption reaction $J_{CO} = J_{SiO}$ and $J_{CO} = -J_{SiO}$, respectively. Our previous work also demonstrated that the rate of reduction of silica to SiC was inversely related to the partial pressure of CO gas. It is

therefore realistic to assume that within the porous mass of silica and carbon kept in a CO ambient atmosphere where P_{CO} is less than the equilibrium value, the diffusion of SiO and CO gas is expected to take place as a result of Reaction 3. On the basis of our previous experiments described elsewhere [7], we have also assumed that the diffusion path of gaseous species is confined to the pellet dimension which was typically a 10 mm × 10 mm cyclinder. This means that the volatilization of SiO occurs within the pore volume where the subsequent carbon reduction (i.e. Reaction 4) must occur. This is diagrammatically shown in Fig. 5. The volatilization of SiO gas and concomitant reduction by carbon can be mathematically describe by a rate process in which the diffusion of CO and SiO gases take place. Therefore, the flux of SiO (J_{SiO}) for the formation of SiO gas via Reaction 3 is

$$J_{SiO,f} = -\frac{PD_{12}}{RT}\left(\frac{dX_{SiO}}{dZ}\right) + X_{SiO}(J_{SiO} + J_{CO}) \quad (5)$$

which from the stoichiometric relationship between the flux of CO and SiO reduces to

$$J_{SiO,f} = -\frac{PD_{12}}{RT}\left(\frac{dX_{SiO}}{dZ}\right) + 2X_{SiO}J_{SiO} \quad (6)$$

where P is the total pressure which in our experimental conditions varied between 0.125 to 1 atm. D_{12} is the interdiffusivity, Z the thickness of the boundary layer, R the universal gas constant and X_{SiO} the mole fraction of SiO gas at a temperature T in the pore volume of a pellet. Equation 6 can be integrated within the limits of X_{SiO} set by Reactions 3 and 4. Hence the upper limit will be determined from Reaction 3, whereas the consumption reaction sets the lower limit of X_{SiO}. The integration of Equation 6 then leads to the equation

$$J_{SiO,f} = 2\frac{PD_{12}}{RTZ}\ln\left(\frac{1 - 2X^{e}_{SiO}}{1 - 2X^{g}_{SiO}}\right) \quad (7)$$

where X^{e}_{SiO} and X^{g}_{SiO} respectively designate the equilibrium mole fractions of this gas from Reactions 3 and 4, respectively. Equation 7 yields finite values of J_{SiO} as long as $X^{g}_{SiO} < 0.5$. At $P_{CO} = 0.125$ atm and 1923 K, the value of X^{g}_{SiO} equals 0.922 which will render this equation an indeterminate quantity. For this reason, the logarithmic term in Equation 7 is expanded and higher orders are neglected. $J_{SiO,f}$ can thus be expressed as

$$J_{SiO,f} = \frac{9.2\,PD_{12}}{RTZ}(X^{g}_{SiO} - X^{e}_{SiO})\left(1 - X^{g}_{SiO} + \frac{(X^{g}_{SiO})^2}{3}\right) \quad (8)$$

Similarly for the consumption of SiO gas, $J_{SiO,c}$ can be derived and is equal to

$$J_{SiO,c} = \frac{PD_{12}}{RTZ}(X^{g}_{SiO} - X^{e}_{SiO}) \quad (9)$$

The overall flux of SiO, $J_{overall}$, can be derived by adding Equations 8 and 9 which leads to Equations 10 and 11 below:

$$J_{overall} = \frac{PD_{12}}{2RTZ}(X^{g}_{SiO} - X^{e}_{SiO}) \times\left\{1 + \left[9.2\left(1 - X^{g}_{SiO} + \frac{(X^{g}_{SiO})^2}{3}\right)\right]\right\} \quad (10)$$

$$J_{overall} = \frac{PD_{12}}{RTZ}X^{g}_{SiO} \times\left[10.2 - 9.2\left(X^{g}_{SiO} - \frac{(X^{g}_{SiO})^2}{3}\right)\right] \quad (11)$$

From Equation 11, the computed value of J_{SiO} has been plotted against the reciprocal temperature in Fig. 6. For this computation, the value of D_{12} was required at each temperature and this was obtained from the interdiffusivity equation cited elsewhere [13, 38]. The value of D_{12} represents the interdiffusivity of SiO gas in an atmosphere of CO. For the total pressure, $P = 0.125$ atm, the computed values of J_{SiO} together with the equilibrium value of X_{SiO} and D_{12} are listed in Table V. Fig. 6 shows that above 1773 K, the concentration term in Equation 11 has a very small effect and for this temperature range the value of the activation energy is of the order of 105 kJ, which is in proximity very similar to that derived from the rate of reduction curves by Chrysanthou *et al.* [7]. Below 1773 K when the pressure of SiO gas decreases, the

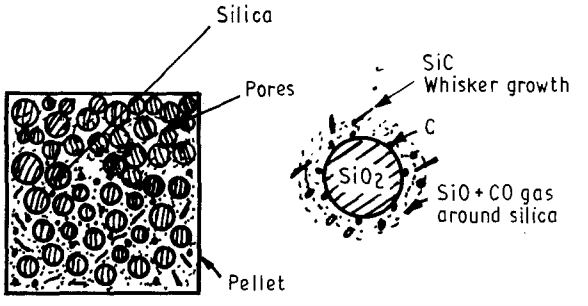

Figure 5 Schematic description of SiO gas formation within the pellet pore volume.

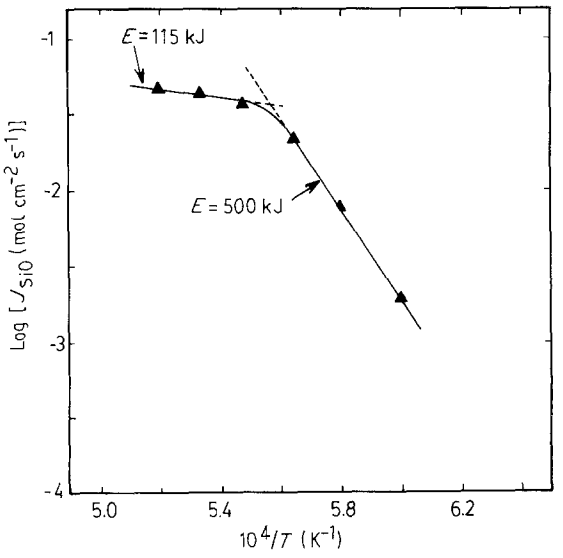

Figure 6 (▲) Plot of $\log J_{SiO}$ against reciprocal temperature, calculated from Equation 11; $P_{CO} = 0.125$ atm. The derived values of E = 115 and 500 kJ compare with the published values of 105 kJ [7] abd 535 kJ [1], respectively.

TABLE V Computed values of $J_{overall}$ for SiO from Equation 11 at various temperatures T and corresponding X^{g}_{SiO} ($Z = 10\ \mu m$, $R = 82.1\ cm^3\ atm\ K^{-1}\ mol^{-1}$, $P = 0.125$ atm)

T (K)	X^{g}_{SiO}	D_{12} ($cm^2\ s^{-1}$)	log [$J_{overall}$ (mol s^{-1})]
1923	0.922	3.68	− 2.236
1873	0.789	3.52	− 2.263
1823	0.526	3.37	− 2.337
1773	0.238	3.22	− 2.567
1723	0.174	3.08	− 3.010
1623	0.081	2.95	− 3.616

rate of reaction also suffers. The derived value of activation energy is of the order of 500 kJ and is comparable to the datum derived by Lee and Cutler [1] for uncatalysed reaction. What we imply from these computed kinetic analyses is that the reaction rate in these temperature regimes is primarily governed by the rate of SiO evolution.

In the light of chemical reactions that determine the vapour pressure of SiO gas, the most important reaction is that of involving the nucleation of CO. The kinetics of CO nucleation determines the formation of SiO, and this was pointed out by Chrysanthou *et al.* [7] where the role of the active form of carbon was recognized. Under a low partial pressure of CO gas the vaporization of SiO will be extensive and neither SiC powder nor whiskers will form. The P_{SiO} versus P_{CO} diagram described elsewhere signifies this aspect [7].

3.2. Silicide liquid–SiC whisker growth kinetics

Formation of an iron–silicon-based liquid has been reported during the growth of SiC whisker by several authors [1–4, 7] and it has been claimed that the iron silicide liquid provides energetically favourable sites for whisker growth. It was also pointed out that due to the evolution of SiO, silicon metal produced in a reducing atmosphere can dissolve in the metallic iron impurities to form an iron–silicon alloy. The addition of either Si in an Fe–C melt or C in an Fe–Si melt results in a substantial decrease in the surface tension of the liquid–SiC interface, which provides a lower energy barrier for nucleation of SiC [2, 7]. The evaluation of phase boundaries using the Clausius–Clapeyron relationship showed that a liquid between SiC and FeSi can exist above 1438 K. Also the measured solubility data for C and Si in liquid iron obtained by Chipman *et al.* [10] shown in Fig. 7 indicates that there might be a ternary liquid at 1460 K which upon solidification produces α-Fe, β-SiC and a silicide phase containing 10–11 wt% Si. In the Fe–Si–C system two melting events occur, one at 1473 K and the other which is recognized as a ternary entectic occurring at 1460 K. This result is 20 K higher than our predicted value obtained from the calculated pseudo-binary phase diagram and observations made by Bootsma *et al.* [2].

The iron–silicon–carbon liquid at a given temperature and pressure is a univariant liquid phase in equilibrium with the gas and β-SiC crystal. This

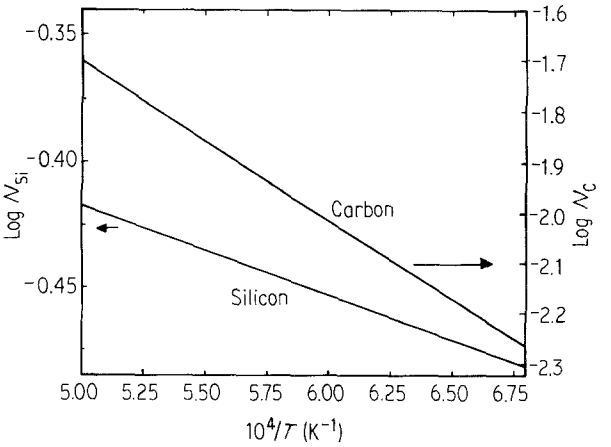

Figure 7 Solubility of C and Si in an Fe–Si–C alloy (after Chipman *et al.* [10]).

means that the composition of the silicide liquid is expected to change particularly with respect to Si and C. From the gas phase, Si and C are transferred to the silicide liquid droplet. When the liquid is saturated with carbon and silicon, the precipitation of SiC takes place and the composition of the liquid momentarily departs from the equilibrium condition. The rejection of SiC from Fe–C–Si liquid is therefore a continuous process and is schematically shown in Fig. 8. The droplet size of Fe–Si–C liquid in equilibrium with SiC is determined by the amount of iron present at these energetically favourable sites. Indeed the volume of this liquid determines the dimensions of the silicon carbide whiskers. This was originally confirmed by Bootsma *et al.* [2].

The constituents of whiskers of SiC are transferred across a liquid–crystal interface and surface-diffuses to build a new layer of SiC along the growth direction. A schematic representation of the ledge-assisted mechanism was given in our earlier work and the mass transport mechanism for the existence of this process will be verified below. The self-diffusion coefficients of silicon and carbon in the β-SiC structure have been measured by Hon and Davis [39, 40] in the temperature range 2128 to 2547 K. It was reported that the self-diffusitives of ^{14}C isotope for both lattice (D^{*lc}) and grain boundary (D^{*bc}) transport (in $cm^2\ s^{-1}$) are given by

$$D^{*lc} = [(2.62 \pm 1.83) \times 10^8] \times \exp\left(-\frac{(8.72 \pm 0.14)}{kT} \text{eV at}^{-1}\right) \quad (12)$$

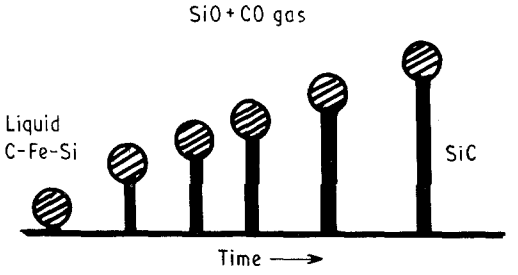

Figure 8 Schematic description of the mechanism of silicon transfer from the gas phase via reduction of the SiO gaseous species, and isothermal rejection of Si and C from Fe–Si–C to form SiC whiskers.

and

$$D^{*bc} = [(4.44 \pm 2.03) \times 10^7] \times \exp\left(-\frac{(5.84 \pm 0.09)}{kT} \text{eV at}^{-1}\right) \quad (13)$$

The self-diffusion coefficient of ^{30}Si isotope in a polycrystalline β-SiC is reported to be equal to

$$D^{*lsi} = [(8.36 \pm 1.99) \times 10^7] \times \exp\left(-\frac{(9.45 \pm 0.05)}{kT} \text{eV at}^{-1}\right) \quad (14)$$

Here 1 eV corresponds to 96.5 kJ. From the diffusion equation shown above, the diffusivity of silicon is expected to be slower than that of the carbon in the β-SiC structure. Jha and Grieveson [31] reported that the equation proposed by Wagner [41] could be satisfactorily employed to describe the whisker growth process which occur under the influence of a chemical potential gradient. The rate of growth or dimensional change, for example l_{corr} (μm s^{-1}) which Bootsma *et al.* recorded, can be defined as in Equation 15 below where $\dot{n}$ is equivalent to l_{corr}. A is the surface area, C_{SiC} is the concentration of Si or SiC at the growth interface and r and F_{SiC} are radius of the whiskers and geometrical parameter, respectively, the latter having a value of unity:

$$\dot{n} = \frac{4AC_{SiC}D^*_{SiC}}{rF_{SiC}} \ln\left(\frac{a^{SP}}{a_o}\right) \quad (15)$$

By using the above equation, we have computed the rate of change of length l_{corr} with the lattice diffusion (D^{*lc}) of carbon and silicon and find that lattice diffusion could not be a major mass transport mechanism to account for such a growth rate. The value of D^*_{SiC} for a given supersaturation condition of Fe–Si–C alloy at an isotherm can be computed provided that the value of the activity ratio a^{SP}/a_o for silicon carbide is known. a^{SP} determines the supersaturation thermodynamic activity of SiC in the Fe–Si–C liquid with respect to the standard equilibrium activity of unity, at which the overall mass transport will reduce to a negligible value. The above equation for mass transport indicates that the diffusion of constituent elements is directly related to the thermodynamic driving force as pointed out by Darken, i.e.

$$D_{chem} = kTB_c \frac{d(\ln a_c)}{d(\ln X_c)} \quad (16)$$

Therefore in Equation 15, $D^*_{SiC} \ln (a^{SP}/a_o)$ represents the mobility (B_C) times the slope of the activity versus concentration curve at a temperature T; k is the Boltzmann constant. The value of the diffusion parameter D^*_{SiC} in the equation can therefore be derived by substituting the value of activity ratio and n in the equation. The calculated values of D^*_{SiC} obtained from the experimental results of Bootsma *et al.* [31] and from our previous work [7] on SiC whiskers are summarized in Table VI. These are plotted against the reciprocal value of absolute temperature in Fig. 9. It is interesting to observe that below 1498 K there appears to be a sharp step above which the logarithimic diffusion parameter varies linearly with the reciprocal of the absolute temperature. The activation energy for the diffusive barrier is equal to 510 kJ compared to 585 kJ for the grain boundary diffusion of silicon carbide reported by Hon and Davis [39]. The discontinuity at the lower-temperature end is due to the phase transition in the temperature range 1460 to 1498 K reported by Chipman *et al.* [10]. The lower value of activation energy means that the mechanism of grain-boundary self-diffusion of C in β-SiC is energetically more difficult than the overall diffusion observed during the growth of SiC whiskers from an Fe–Si–C liquid. This difference may be chiefly due to the existence of a chemical potential gradient that enhances the diffusion rates.

TABLE VI Estimated values of D^*_{SiC} from the whisker growth rate data using Equation 15

T (K)	$\dot{n}_{SiC}$ (cm s^{-1})	$\ln a_{SiC}$	D^*_{SiC} (cm^2 s^{-1})
1473	1.33×10^{-7}	4.20	2.88×10^{-17}
1498	1.66×10^{-7}	4.01	3.77×10^{-17}
1523	3.33×10^{-6}	3.79	7.99×10^{-16}
1548	5.8×10^{-6}	3.61	1.46×10^{-15}
1573	8.33×10^{-6}	3.38	2.24×10^{-15}
1673	1.05×10^{-5}	2.76	1.91×10^{-14}
1723	5.2×10^{-5}	2.47	1.17×10^{-13}

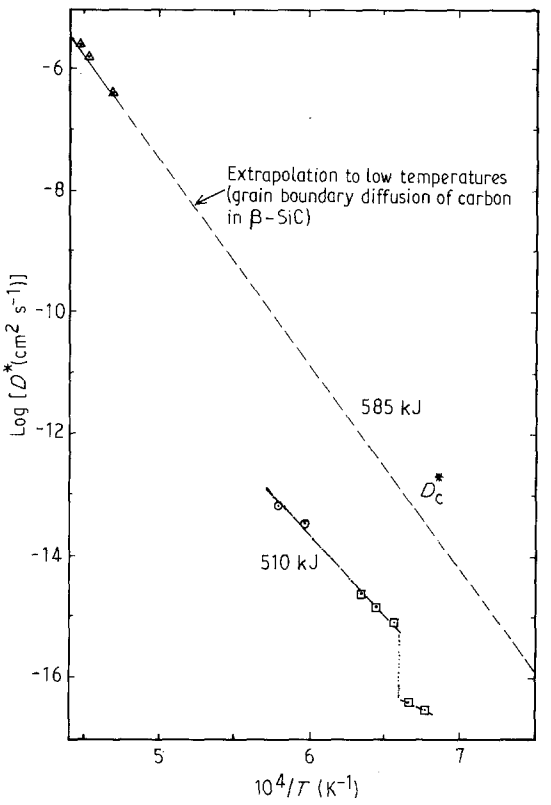

Figure 9 Temperature dependence of the diffusivity of carbon, D^*_{SiC}, for β-SiC whisker growth: (⊙) Chrysanthou *et al.* [7], (⊡) Bootsma *et al.* [32], (△) Hon and Davis [39].

4. Conclusions

1. The calculated free energy of α-Si_3N_4 agrees satisfactorily with the empirical values, particularly in the lower temperature range.

2. The α-SiC phase is more stable at higher oxygen potential than the β-SiC. This is evident from the recalculated Si–C–N–O phase boundaries.

3. The calculated value of J_{SiO} indicates that the rate of silicon oxide reduction to β-SiC is strongly dependent upon the partial pressure of the SiO gas.

4. The temperature dependence of D^*_{SiC} for whisker growth suggests that the rate of carbon diffusion during β-SiC whisker growth is a surface-diffusion controlled process.

References

1. J. G. LEE and I. B. CUTLER, *Ceram. Bull.* **54** (1975) 195.
2. G. A. BOOTSMA, W. F. KNIPPENBERG and G. VERSPUI, *J. Cryst. Growth* **11** (1971) 297.
3. J. V. MILEWSKI, F. D. GAC, J. J. PETROVIC and S. R. SKAGGS, *J. Mater. Sci.* **20** (1985) 1060.
4. Y. W. CHO and J. A. CHARLES, *Mater. Sci. Technol.* **7** (1991) 289.
5. S. A. SIDDIQI, I. HIGGINS and A. HENDRY, in "Non-oxide Technical and Engineering Ceramics", edited by S. Hampshire (Elsevier Applied Science, Stoke-on-Trent 1986) p. 119.
6. H. SAITO and I. YAMAI, *J. Ceram. Soc. Jpn* **88** (1980) 265.
7. A. CHRYSANTHOU, P. GRIEVESON and A. JHA, *J. Mater. Sci.* **26** (1991) 3463.
8. H. WADA, M-J. WANG and T-Y. TIEN, *J. Amer. Ceram. Soc.* **71** (1988) 837.
9. M. J. WANG and H. WADA, *Mater. Sci. Forum* **47** (1989) 267.
10. J. CHIPMAN, J. C. FOULTON, N. GOCKEN and G. R. CASKEY Jr. *Acta Metall.* **2** (1954) 439.
11. J. R. O'CONNOR and J. SMILENS (eds), "Silicon Carbide. A High Temperature Semiconductor", (Pergamon, London, 1960) p. 1.
12. J. DROWART and G. De MARIA, *ibid.* p. 16.
13. E. T. TURKDOGAN, "The Physical Chemistry of High Temperature Technology" (Academic, London, 1980) p. 20.
14. R. I. SCACE and G. A. SLACK, in "Silicon Carbide. A High Temperature Semiconductor", edited by J. R. O'Connor and J. Smilens (Pergamon, London, 1960) p. 24.
15. F. A. HALDEN, *ibid.* p. 115.
16. R. D. PEHLKE and J. F. ELLIOTT, *Trans. Metall. Soc.* **67** (1971) 2945.
17. S. WILD, P. GRIEVESON and K. H. JACK, in "Special Ceramics 5", edited by P. Popper (British Ceramic Research Association, Stoke-on-Trent, 1972) p. 271.
18. W. A. KRIVSKY and R. SCHUHMANN Jr, *TMS-AIME* **21** (1961) 898.
19. T. ROSENQVIST, "Principles of Extractive Metallurgy" (McGraw-Hill, New York, 1983) p. 411.
20. A. SCHEI, *Tidsskr. Kjemi Bergr. Metall.* **27** (1967) 152.
21. J. J. RITTER, *Proc. Mater. Res. Soc. Symp.* **73** (1986) 367.
22. S. YAJIMA, J. HAYASHI, M. OMORI and K. OKAMURA, *Nature* **261** (1976) 683.
23. S. SHINOZAKI and K. R. KINGMAN, *Acta Metall.* **26** (1978) 769.
24. L. U. OGBUJI, T. E. MITCHELL and A. H. HEUER, *J. Amer. Ceram. Soc.* **64** (1981) 91.
25. I. COLQUHOUN, S. WILD, P. GRIEVESON and K. H. JACK, in Proceedings of British Ceramic Society, edited by D. J. Godfrey (British Ceramic Society, Stoke-on-Trent, 1973) p. 207.
26. S. WILD, P. GRIEVESON and K. H. JACK, in "Special Ceramics 5", edited by P. Popper (British Ceramic Research Association, Stoke-on-Trent, 1972) p. 385.
27. J. LI, G. PENG, S. CHEN, Z. CHEN and J. WU, *J. Amer. Ceram. Soc.* **73** (1990) 919.
28. R. De JONG, R. A. McCAULEY and P. TAMBUYSER, *ibid.* **70** (1987) C338.
29. N. SETAKA and K. EJIRI, *ibid.* **52** (1969) 60.
30. L. F. ALLARD, P. PENDLETON and J. S. BRINEN, in Proceedings of 44th Annual Meeting of Electron Microscopy Society of America, edited by G. W. Bailey (San Francisco Press, San Francisco, 1986) p. 472.
31. A. JHA and P. GRIEVESON, *J. Mater. Sci.* **25** (1990) 2299.
32. G. A. BOOTSMA, W. F. KNIPPENBERG and G. VERSPUI, *J. Cryst. Growth* **8** (1971) 341.
33. L. V. OGBUJI, T. E. MITCHELL and A. H. HEUER, *J. Amer. Ceram. Soc.* **64** (1981) 100.
34. H. SATO, S. SHINOZAKI and M. YESSIK, *J. Appl. Phys.* **45** (1974) 1630.
35. S. AMELINCKX and G. STRUMANE, in "Silicon Carbide. A High Temperature Semiconductor", edited by J. R. O'Connor and J. Smilens (Pergamon, London, 1960). p. 192.
36. I. COLQUHOUN, D. P. THOMPSON, W. I. WILSON, P. GRIEVESON and K. H. JACK, in Proceedings of British Ceramic Society, edited by D. J. Godfrey (British Ceramic Society, Stoke-on-Trent, 1973) p. 181.
37. W. Y. SUN, P. A. WALLS and D. P. THOMSON, in "Non-oxide Technical and Engineering Ceramics, edited by S. Hampshire (Elsevier Applied Science, 1986) p. 105.
38. E. T. TURKDOGAN, "The Physical Chemistry of High Temperature Technology (Academic, London, 1980) p. 202.
39. M. H. HON and R. F. DAVIS, *J. Mater. Sci.* **14** (1979) 2411.
40. M. H. HON, R. F. DAVIS and D. E. NEWBURY, *ibid.* **15** (1980) 2073.
41. C. WAGNER, in "The Physical Chemistry of Steel Making – The Chipman Conference", edited by J. F. Elliott (MIT Press, Cambridge, 1962) p. 19.

Received 29 June
and accepted 17 November 1992